405

FILE COPY
NO 1

CONFIDENTIAL

Copy No. 175
RM No. L8G30

NACA RM No. L8G30

NACA
CASE FILE
COPY

RESEARCH MEMORANDUM

LONGITUDINAL STABILITY AND CONTROL CHARACTERISTICS OF A SEMISPAN MODEL OF A SUPERSONIC AIRPLANE CONFIGURATION AT TRANSONIC SPEEDS FROM TESTS BY THE NACA WING-FLOW METHOD

By

Norman S. Silsby and James M. McKay

Langley Aeronautical Laboratory
Langley Field, Va.

THIS DOCUMENT ON LOAN FROM THE FILES OF

NATIONAL ADVISORY COMMITTEE FOR AERONAUTICS
LANGLEY AERONAUTICAL LABORATORY
LANGLEY FIELD, HAMPTON, VIRGINIA

RETURN TO THE ABOVE ADDRESS.

REQUESTS FOR PUBLICATIONS SHOULD BE ADDRESSED AS FOLLOWS:

NATIONAL ADVISORY COMMITTEE FOR AERONAUTICS
1512 H STREET, N. W.
WASHINGTON 25, D. C.

CLASSIFIED DOCUMENT

This document contains classified information affecting the National Defense of the United States within the meaning of the Espionage Act, USC 50:31 and 32. Its transmission or the revelation of its contents in any manner to an unauthorized person is prohibited by law. Information so classified may be imparted only to persons in the military and naval services of the United States, appropriate civilian officers and employees of the Federal Government who have a legitimate interest therein, and to United States citizens of known loyalty and discretion who of necessity must be informed thereof.

RETURN TO LIBRARY OF LANGLEY AERONAUTICAL LABORATORIES

CLASSIFICATION CHANGED TO UNCLASSIFIED DATE 8-18-54
AUTHORITY J.W.CROWLEY
CHANGE # 2393 W.H.L.

NATIONAL ADVISORY COMMITTEE FOR AERONAUTICS

WASHINGTON
November 8, 1948

CONFIDENTIAL

32

NATIONAL ADVISORY COMMITTEE FOR AERONAUTICS

RESEARCH MEMORANDUM

LONGITUDINAL STABILITY AND CONTROL CHARACTERISTICS OF A SEMISPAN MODEL OF A SUPERSONIC AIRPLANE CONFIGURATION AT TRANSONIC SPEEDS FROM TESTS BY THE NACA WING-FLOW METHOD

By Norman S. Silsby and James M. McKay

SUMMARY

An investigation has been made by the NACA wing-flow method to determine the longitudinal stability and control characteristics at transonic speeds of a semispan airplane model having a long slender fuselage and a straight wing and tail of low aspect ratio with faired symmetrical double-wedge airfoil sections 4.6 percent of the chord in thickness. Measurements were made of the normal force and pitching moment at various angles of attack of the model with five different angles of incidence of the stabilizer. The tests were made at effective Mach numbers at the wing of the model from 0.56 to 1.13.

Over the entire range of Mach numbers tested, the results indicated fairly gradual changes in aerodynamic characteristics up to a normal-force coefficient of 0.4. The neutral point moved back from 38 percent mean aerodynamic chord to 56 percent mean aerodynamic chord as the Mach number increased from 0.8 to 1.10. The stabilizer was effective in changing the pitching moment throughout the Mach number range for all stabilizer angles tested.

INTRODUCTION

The numerous current designs of airplanes intended to fly at transonic and supersonic speeds include a variety of wing-fuselage-tail configurations. There is, as yet, little or no information on the aerodynamic characteristics of most of these configurations at transonic speeds. In the investigation of what is considered the more basic of such configurations, tests were made at transonic speeds by the NACA wing-flow method to determine the longitudinal stability and control characteristics of a semispan model of a supersonic configuration. The model tested incorporated a very slender fuselage, low-aspect-ratio unswept wing and tail with thin sharp-leading-edge airfoil sections. The horizontal tail of the model is of the all-movable type. Measurements were made of the normal force and

pitching moment at various angles of attack of the semispan model with the stabilizer set at five different angles of incidence. The tests covered a range of effective Mach numbers at the wing of the model from 0.56 to 1.13.

SYMBOLS

α angle of attack of fuselage, degrees

i_t incidence of stabilizer, degrees

M_L local Mach number at wing surface of P-51D airplane

M_w effective Mach number at wing

M_t effective Mach number at tail

q effective dynamic pressure, pounds per square foot $\left(\frac{1}{2}\rho V^2\right)$

S wing area, semispan, square feet

$\bar{c}$ mean aerodynamic chord of wing; based on the relationship

$\int_0^{b/2} \frac{c^2\,dy}{S}$ where b is wing span and c is chord, inches

N normal force, pounds

M pitching moment, inch-pounds

C_N normal-force coefficient (N/qS)

$C_{M_{0.50c}}$ pitching-moment coefficient referred to $0.50\bar{c}$ $(M/qS\bar{c})$

R_w Reynolds number of wing based on mean aerodynamic chord $\bar{c}$

R_t Reynolds number of tail based on mean aerodynamic chord of tail

$\left(\frac{dC_N}{d\alpha}\right)_m$ mean slope of normal-force curve per degree for C_N from 0 to 0.2

$\frac{dC_M}{dC_N}$ slope of pitching-moment curve, referred to $0.20\bar{c}$ center-of-gravity location at normal force for trim

APPARATUS AND TESTS

The tests were made, as described in references 1 and 2, by the NACA wing-flow method in which the model is mounted in the high-speed flow over the wing of a P-51D airplane.

Photographs of the semispan model equipped with an end plate at the fuselage center line are given as figures 1 and 2. The geometric characteristics of the model are given in table I; other details of the model are shown in figure 3. Both wing and tail have a taper ratio of 2.0 and airfoil sections 4.6-percent-chord thick which were obtained by fairing a 5-percent-chord-thick symmetrical double-wedge section with a circular arc at midchord. The aspect ratio of the wing, when the airplane wing surface was considered as a reflection plane, was 4.0. The model was mounted close to the airplane wing; and the shank of the model, which passed through a slot in the airplane wing, was mounted on a strain-gage balance. Because the model and balance were arranged to oscillate as a unit, the balance measured the force normal to the chord of the model at all angles of attack. With the model equipped successively with five interchangeable stabilizers having fixed incidences of 0°, 2°, 4°, -2°, and -4°, continuous measurements were made of angle of attack, normal force, and pitching moment about the 50-percent-chord line of the wing as the model was oscillated through an angle-of-attack range of -3° to 11°. The model oscillated at an angular velocity of about 20° per second. A free-floating vane, shown in figure 2, was used to determine the direction of air flow at the model location, as described in reference 3.

The chordwise velocity gradients in the test region on the airplane, as determined from static-pressure measurements at the wing surface with the model removed, are indicated in figure 4. The effective dynamic pressure q, the effective Mach number at the model wing M_w, and the effective Mach number at the model tail M_t, were determined from an integration of the velocity distribution over the area covered by the wing and tail of the model, respectively. The variation of Mach number at the tail M_t with Mach number at the wing M_w, due to the chordwise velocity gradient, is shown in figure 5. A more complete discussion of the method of determining the Mach number and dynamic pressure at the model can be found in reference 3.

The tests were made in two high-speed dives of the P-51D airplane, one from 28,000 to 21,000 feet, the other from 18,000 to 12,000 feet, and in a low-altitude (5000 feet) high-speed level-flight run, to obtain different ranges of Reynolds number. The average relation between Reynolds number at the wing R_w and the Reynolds number at the tail R_t with the Mach number at the wing M_w for the three altitude conditions is shown in figure 6.

RESULTS AND DISCUSSION

The variation of angle of attack with Mach number at constant normal-force coefficients is shown in figure 7 for several stabilizer incidences. These curves were obtained by fairing data similar to that which is shown as a sample in figure 8. The scatter of the data in figure 8 resulted principally from the differences in time lag in the recording of the angle of attack and the normal force as the model was oscillated through the range of angles of attack; the differences in time lag occur as a result of differences in damping in the electrical recording circuits. The data of figure 8 show that over the range of Reynolds number covered in the tests there appeared to be no effect of Reynolds number (within experimental error) on angle of attack at a constant normal-force coefficient. Hence the faired data presented in figure 7 were taken from the tests at the lowest Reynolds numbers since these tests covered the highest Mach numbers. The variation of angle of attack with Mach number at a constant normal-force coefficient was somewhat irregular but showed no abrupt changes.

The variation of normal-force coefficient with angle of attack for each stabilizer incidence, shown in figure 9 for several Mach numbers, is essentially linear up to a normal-force coefficient of 0.65. At a normal-force coefficient of 0.65 and higher, and this was evaluated only for the 2° stabilizer incidence, there is a large decrease in the slope of the normal-force curve for a Mach number of 0.75, which disappeared at higher Mach numbers. The slope of the normal-force curve $\left(\frac{dC_N}{d\alpha}\right)_m$ taken over a range of normal-force coefficients from 0 to 0.2 and presented in figure 10, increases fairly gradually but somewhat irregularly with Mach number up to a Mach number of 0.95 for all stabilizer incidences. Above a Mach number of 0.95, $\left(\frac{dC_N}{d\alpha}\right)_m$ decreases fairly gradually for all stabilizer incidences up to the highest Mach number attained.

The variation of pitching-moment coefficient with Mach number is shown in figure 11 for stabilizer incidences from -4° to 4° and for normal-force coefficients from -0.2 to 0.6. Typical data points are shown for the three ranges of Reynolds number only for zero-normal-force coefficient (fig. 11(a)). Faired data for the three ranges of Reynolds numbers are presented in figure 12 as a plot of pitching-moment coefficient against stabilizer incidence for various Mach numbers and zero-normal-force coefficient and in figure 13 as a plot of pitching-moment coefficient against normal-force coefficient for 2° stabilizer incidence and various Mach numbers.

There appears to be only a slight effect of Reynolds number on stabilizer effectiveness (fig. 12) and an appreciable effect on

longitudinal stability (fig. 13) at Mach numbers near 0.87, particularly for negative normal-force coefficients. Since the lower Reynolds number tests extended to higher Mach numbers, the faired data for these tests are presented in figure 11 and subsequent figures. The pitching-moment coefficients (figs. 11 and 12) for a constant stabilizer angle show a large but fairly gradual and irregular variation with Mach number over the entire speed range for normal-force coefficients up to 0.4. At a normal-force coefficient of 0.6, the variation in pitching moment with Mach number is more abrupt.

The variation of pitching-moment coefficient with normal-force coefficient is presented in figure 14 for various stabilizer incidences at several Mach numbers. A cross plot of these data is presented in figure 15 to show the variation of pitching-moment coefficient with stabilizer incidence at various Mach numbers and normal-force coefficients. These results indicate that, for the entire range of stabilizer incidences and for normal-force coefficients up to 0.6, the stabilizer is effective in changing the pitching moment and the stabilizer effectiveness is essentially constant throughout the Mach number range.

Plotted against Mach number in figure 16 are the stabilizer angles required to trim a full-scale airplane in level flight and the slope of the pitching-moment curve $\frac{dC_M}{dC_N}$ where the pitching moment was computed about a center-of-gravity location of 20 percent mean aerodynamic chord. The slope $\frac{dC_M}{dC_N}$ was taken for stabilizer angles for trim and over a range of normal-force coefficients corresponding to $\pm\frac{1}{4}g$ from the normal-force coefficients (also shown in fig. 16) required for level flight at 35,000 feet altitude with an airplane having a wing loading of 90. The scale for the neutral point is also shown in figure 16. The variation of $\frac{dC_M}{dC_N}$ with Mach number indicates that the static margin (the difference between the neutral point and the center of gravity at 20 percent mean aerodynamic chord) decreases from about 31 percent at a Mach number of 0.7 to about 18 percent between the Mach numbers of 0.8 and 0.9, and then increases to a maximum value of about 36 percent mean aerodynamic chord at the highest Mach number attained, 1.10. The large static margin at the lower Mach numbers is probably associated with the beginning of wing stall. The full-scale airplane apparently could be trimmed in level flight at a Mach number from 0.7 to 1.10 with a gradual change in stabilizer angle covering a range of about 2.5°. The variation of stabilizer angle required for trim with Mach number was stable up to a Mach number of 1.03 and was slightly unstable at higher Mach numbers.

In addition to the effects of the low Reynolds numbers of the tests, the results in terms of full-scale flight conditions are subject to some uncertainty because of the difference in the Mach number of the flow at the wing and at the tail, particularly above a Mach number of 1.08. (Refer to fig. 5.)

CONCLUDING REMARKS

The results of NACA wing-flow tests of the longitudinal stability and control characteristics of a semispan model of a supersonic airplane configuration indicated fairly gradual changes in aerodynamic characteristics up to a normal-force coefficient of 0.4 and over the entire range of Mach numbers tested, 0.56 to 1.13. The neutral point moved back from 38 percent mean aerodynamic chord to 56 percent mean aerodynamic chord as the Mach number increased from 0.8 to 1.10. The stabilizer was effective in changing the pitching moment throughout the Mach number range for all stabilizer angles tested. On the basis of the results, the full-scale airplane apparently could be trimmed in level flight at Mach numbers from 0.7 to 1.10 with a gradual change in stabilizer angle covering a range of about 2.5°. The variation of stabilizer angle required for trim with Mach number was stable up to a Mach number of 1.03 and was slightly unstable at higher Mach numbers. For the range of Reynolds number covered, there appeared to be only a slight effect of Reynolds number on stabilizer effectiveness but an appreciable effect on longitudinal stability at Mach numbers near 0.87, particularly for negative normal-force coefficients.

Langley Aeronautical Laboratory
National Advisory Committee for Aeronautics
Langley Field, Va.

REFERENCES

1. Zalovcik, John A., and Sawyer, Richard H.: Longitudinal Stability and Control Characteristics of a Semispan Airplane Model at Transonic Speeds from Tests by the NACA Wing-Flow Method. NACA ACR No. L6E15, 1946.

2. Zalovcik, John A., and Sawyer, Richard H.: Longitudinal Stability and Control Characteristics of a Semispan Airplane Model with a Swept-Back Tail from Tests at Transonic Speeds by the NACA Wing-Flow Method. NACA RM No. L6K21, 1946.

3. Johnson, Harold I.: Measurements of Aerodynamic Characteristics of a 35° Sweptback NACA 65-009 Airfoil Model with $\frac{1}{4}$-Chord Plain Flap by the NACA Wing-Flow Method. NACA RM No. L7F13, 1947.

TABLE I

GEOMETRIC CHARACTERISTICS OF SEMISPAN MODEL OF

SUPERSONIC AIRPLANE CONFIGURATION

Wing:	
Section	Faired double wedge
Thickness-chord ratio, percent	4.6
Semispan, inches	3.44
Mean aerodynamic chord, inches	1.79
Chord at tip, inches	1.15
Chord at plane of symmetry, inches	2.30
Area (semispan), square inches	5.94
Aspect ratio	4.0
Taper ratio	2:1
Dihedral, degrees	0
Incidence, degrees	0
Horizontal Tail:	
Section	Faired double wedge
Thickness-chord ratio, percent	4.6
Semispan, inches	1.75
Mean aerodynamic chord, inches	.89
Chord at tip, inches	.57
Chord at plane of symmetry, inches	1.15
Area (semispan), square inches	1.50
Aspect ratio	4.0
Taper ratio	2:1
Dihedral, degrees	10
Fuselage length, inches	14.15
Tail length (center line of wing to center line of tail), inches	5.74

NACA

CONFIDENTIAL

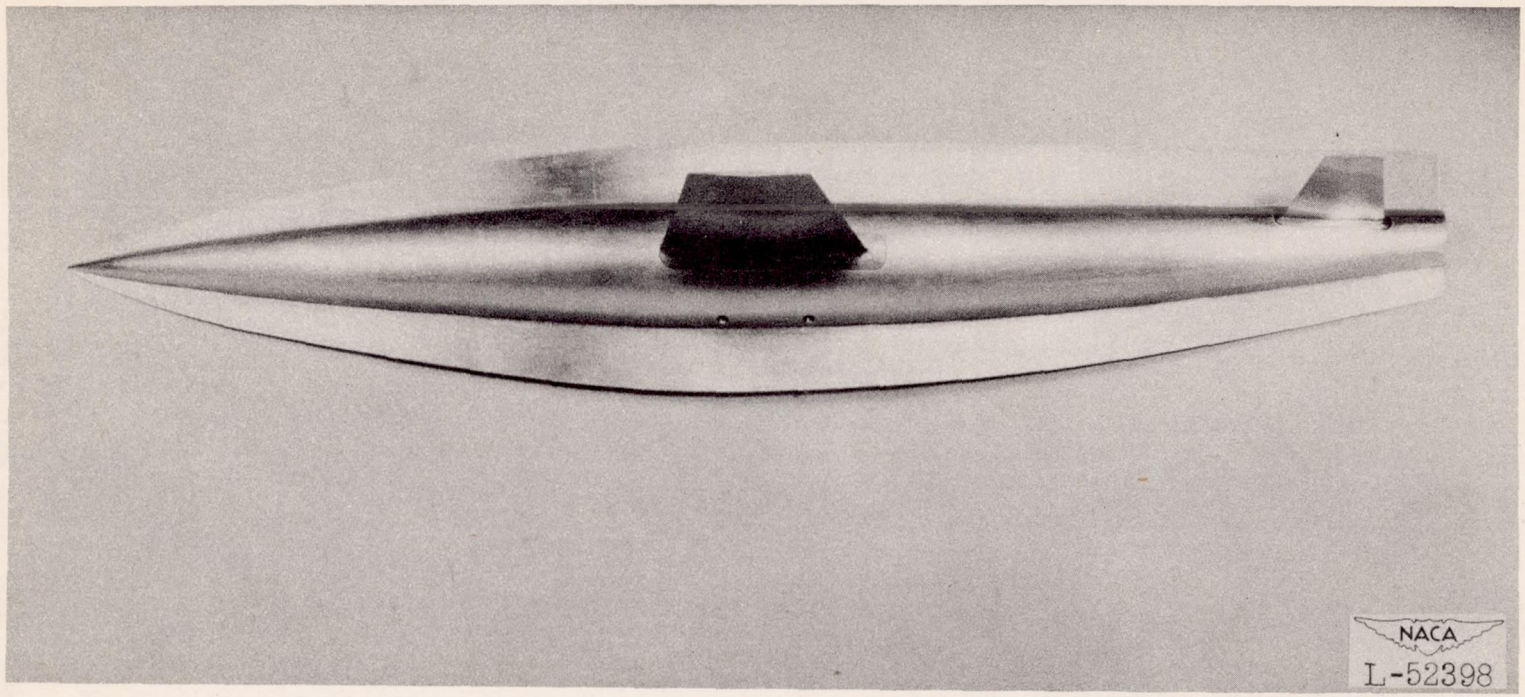

Figure 1.- Semispan model of supersonic airplane configuration.

CONFIDENTIAL

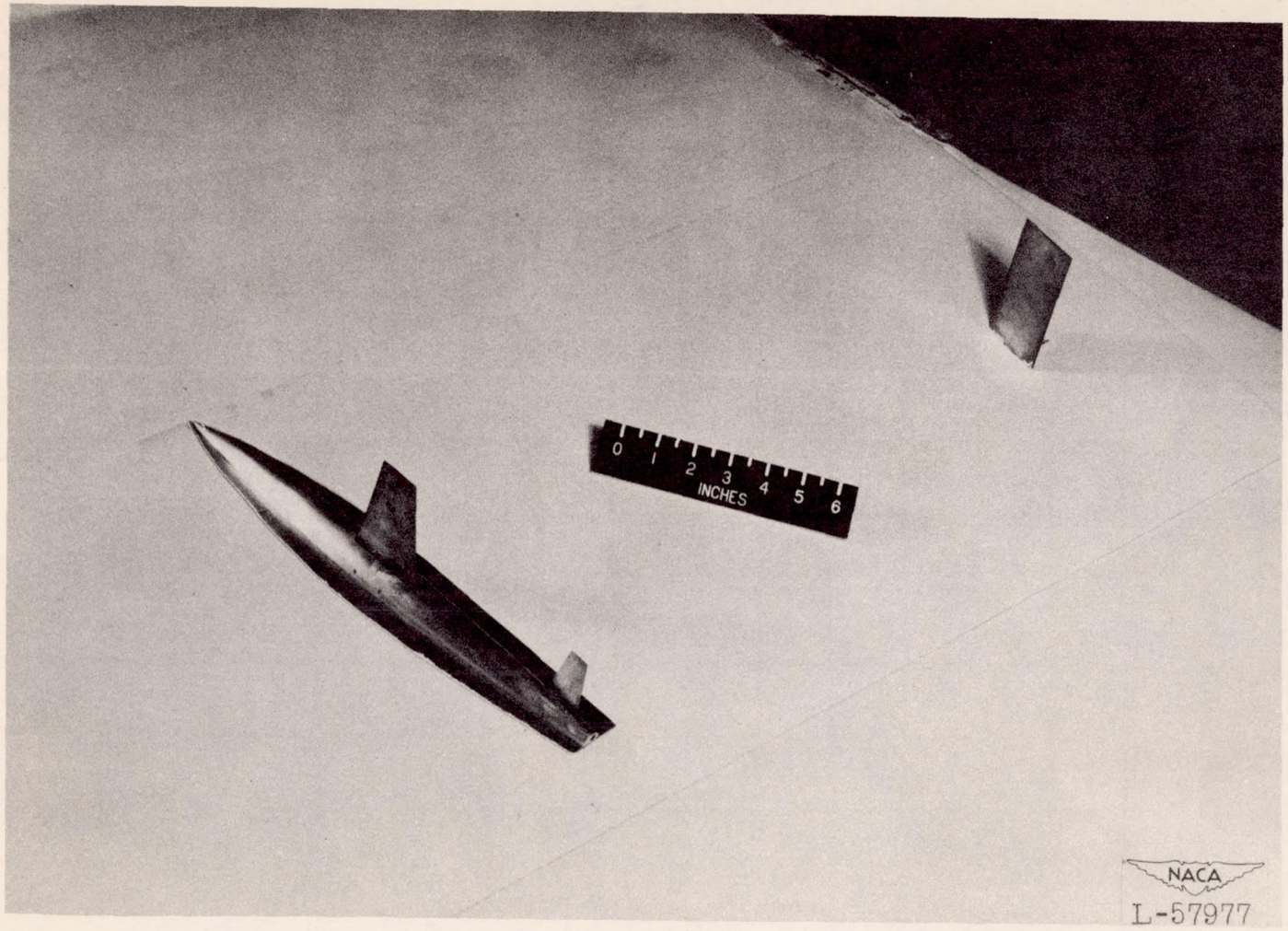

Figure 2.- Semispan supersonic airplane model mounted on wing of P-51D airplane. Free-floating vane also shown.

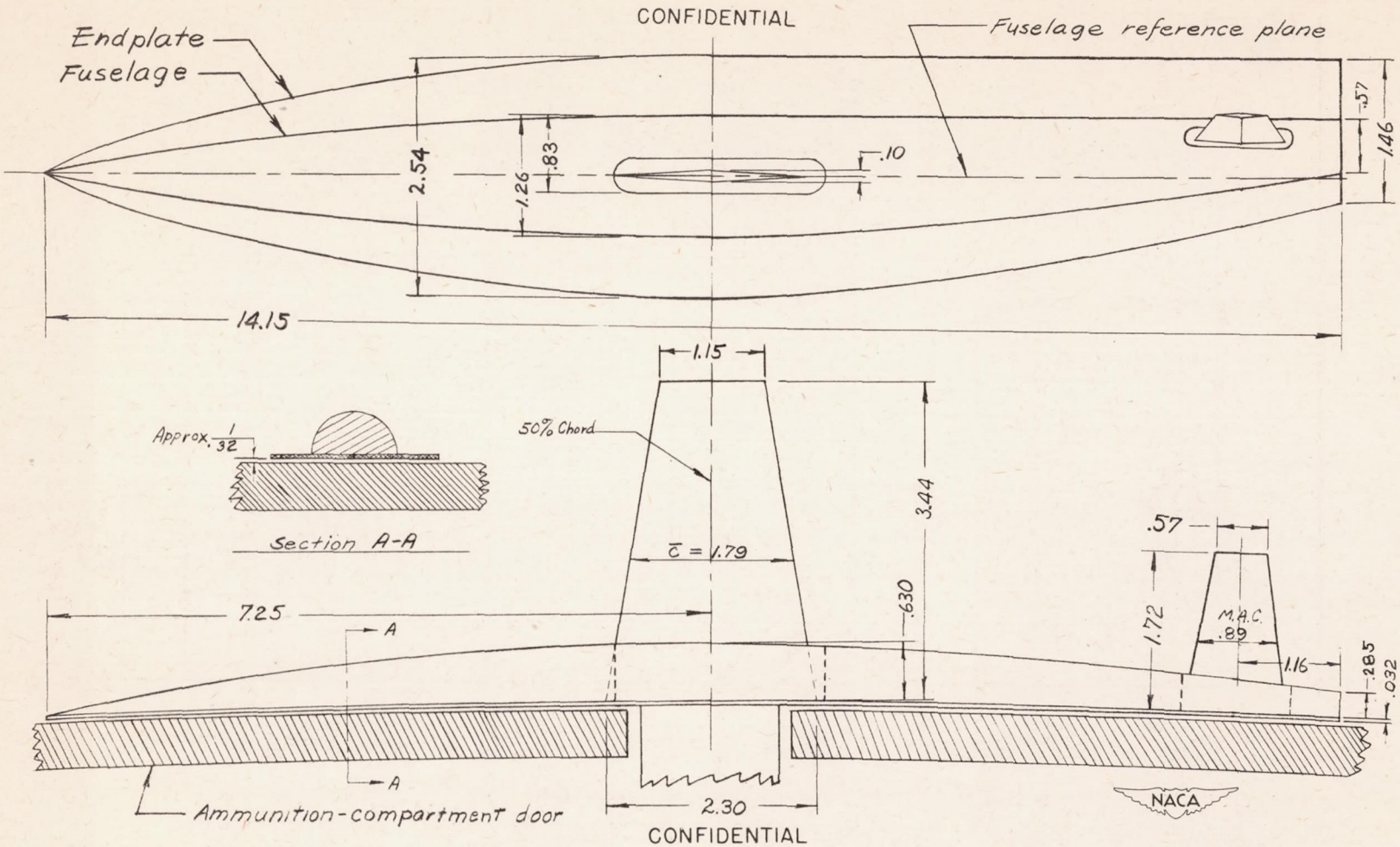

Figure 3.- Details of semispan model of supersonic airplane configuration. (All dimensions are in inches.)

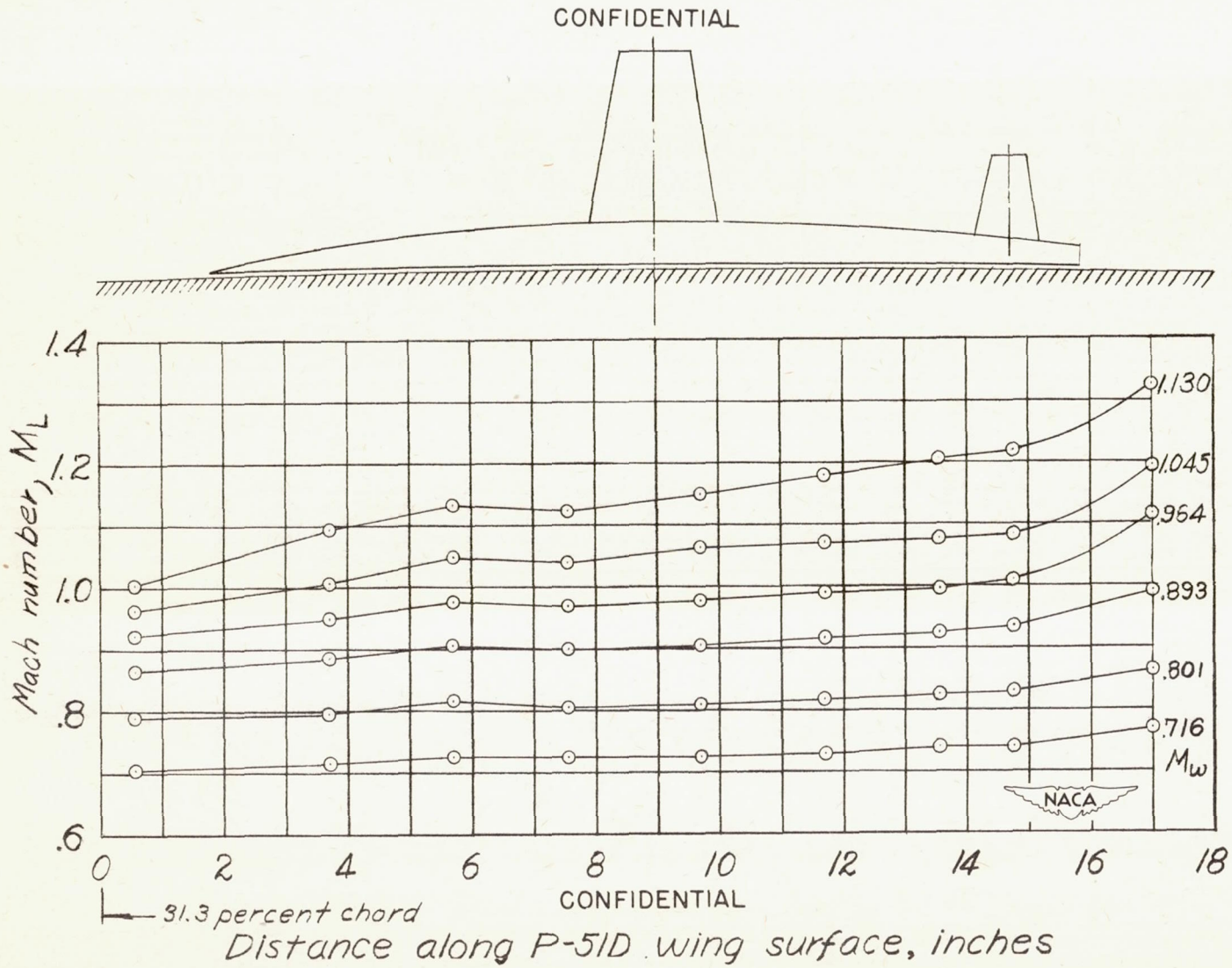

Figure 4.- Typical chordwise variation of Mach number in the test region on the surface of the airplane wing for several Mach numbers at the wing of the model. Chordwise location of model also shown.

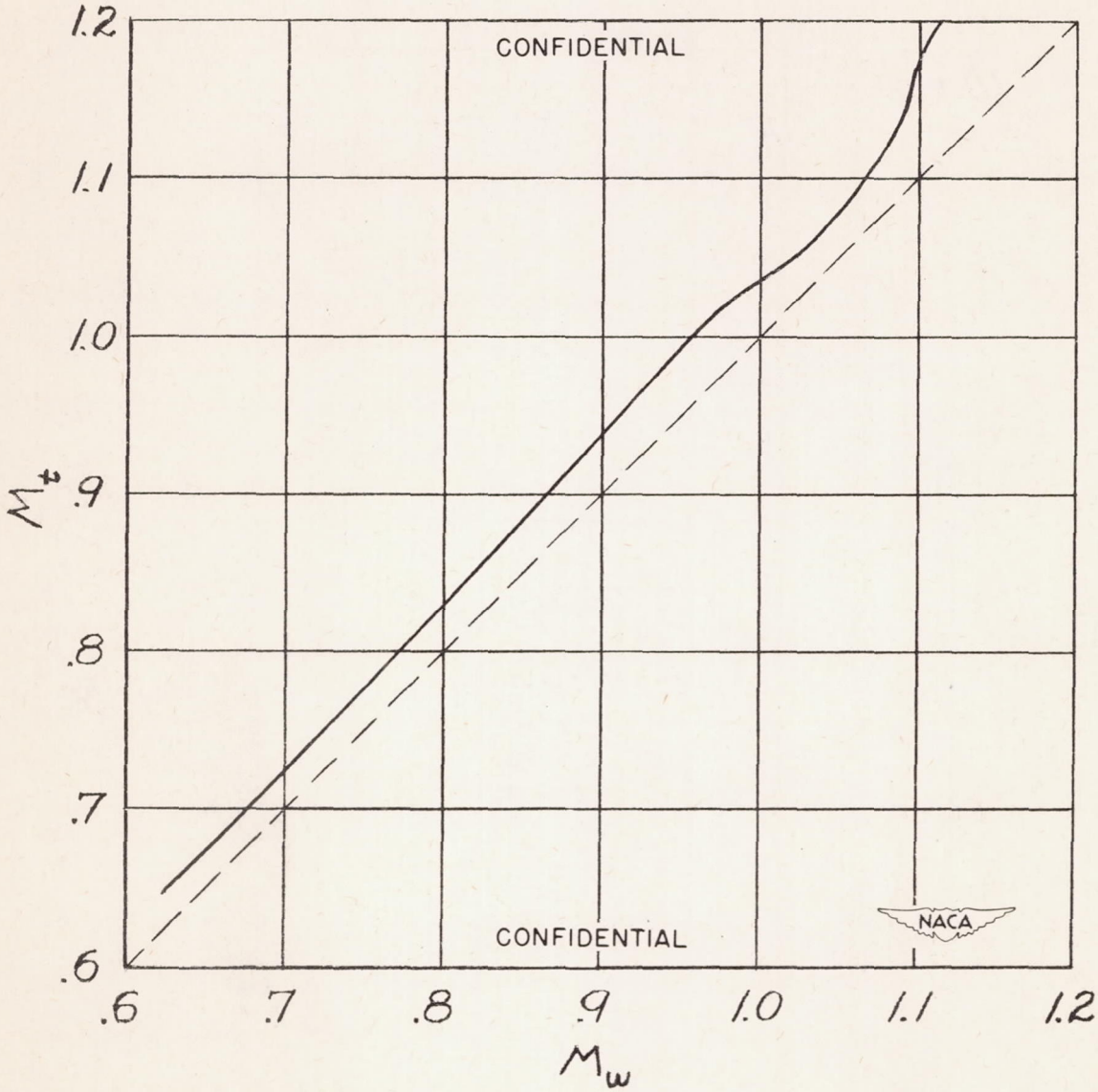

Figure 5.- Variation of Mach number at the tail M_t with Mach number at the wing M_w. Line of agreement shown dotted.

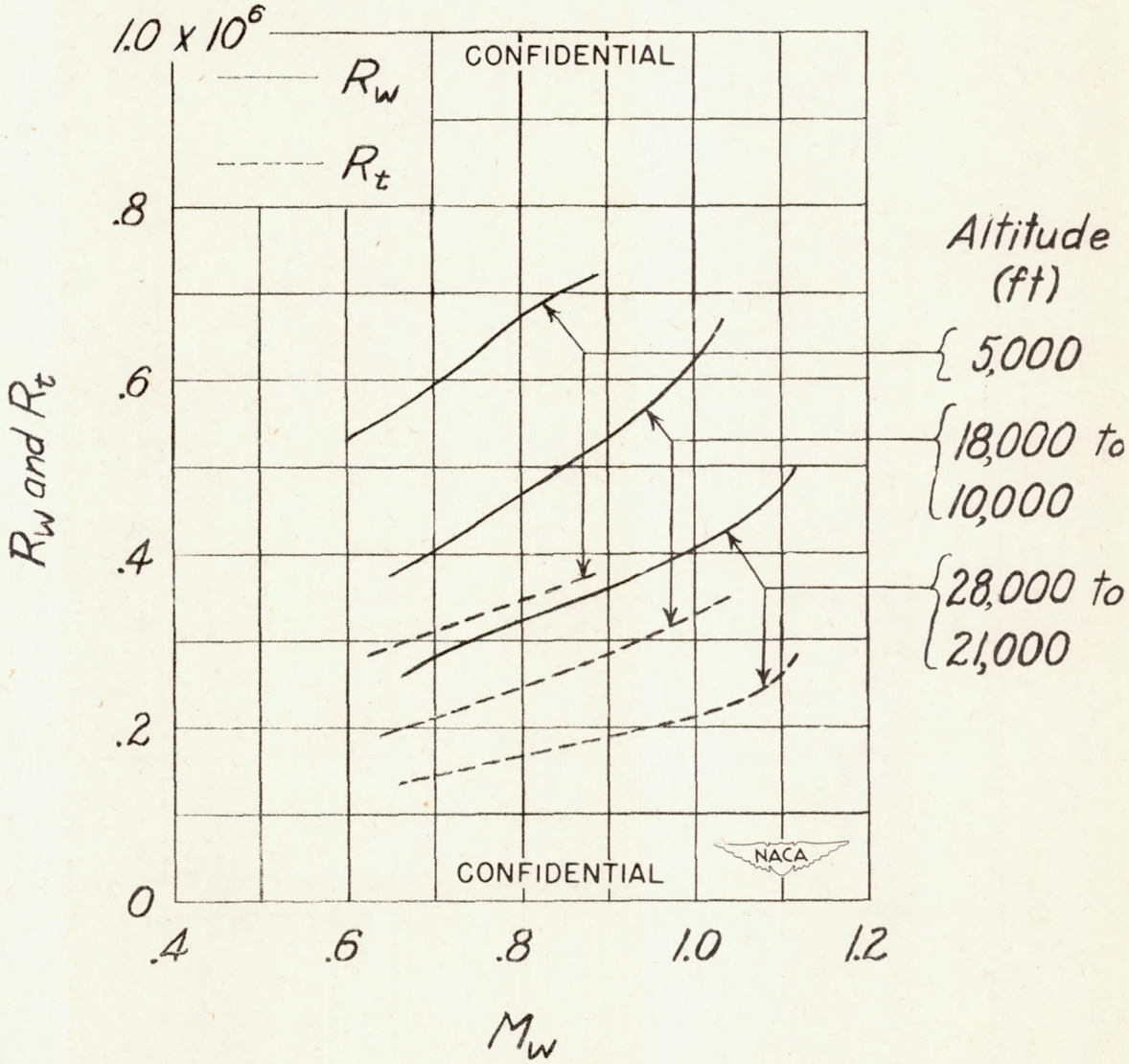

Figure 6.- Variation of Reynolds number of wing R_W and Reynolds number of tail R_t with Mach number for tests at three ranges of altitude.

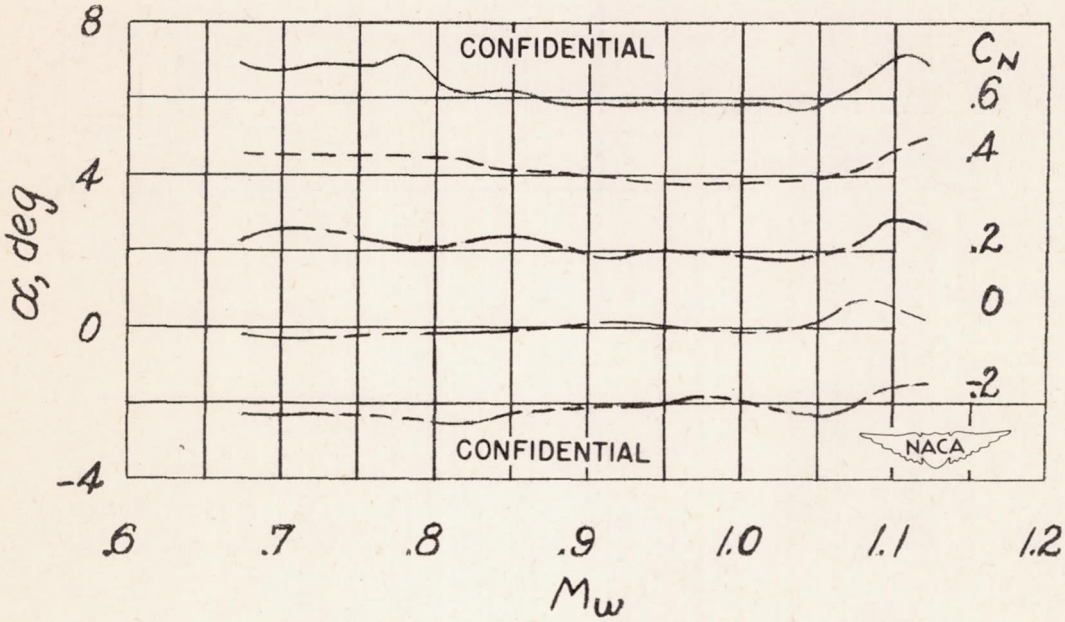

(a) $i_t = 0^{\circ}$.

Figure 7.- Variation with Mach number of angle of attack for several normal-force coefficients at various stabilizer incidences.

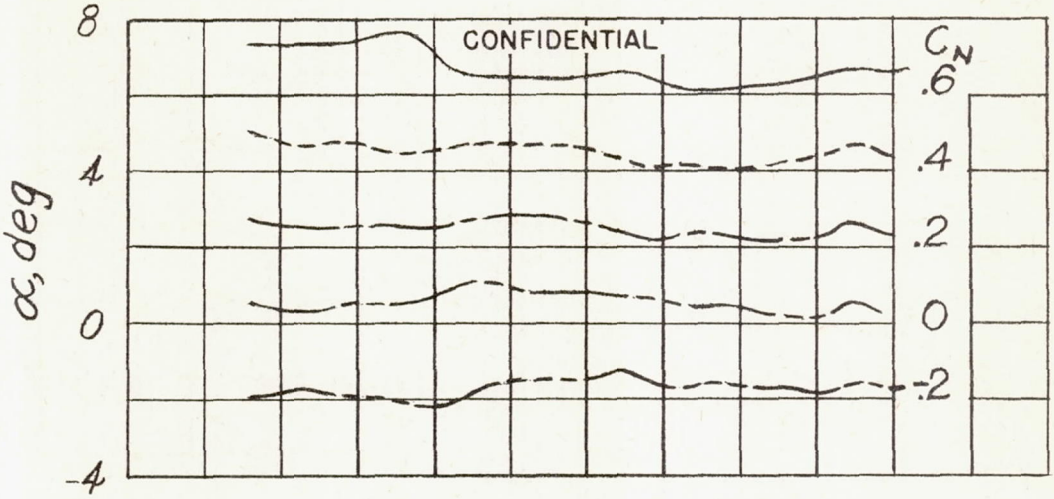

(b) $i_t = -2^{\circ}$.

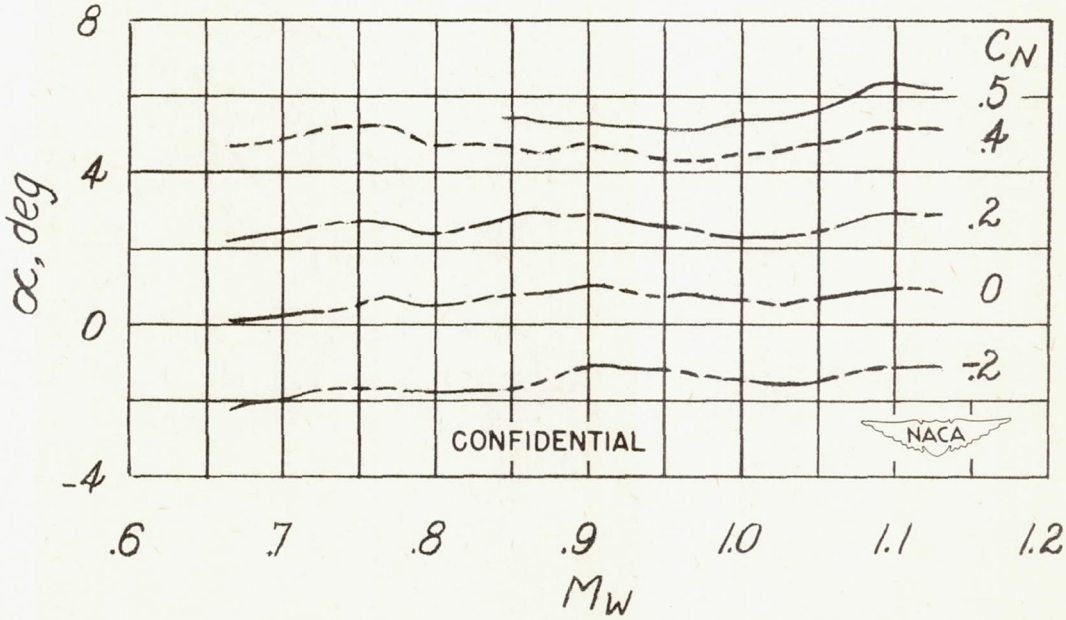

(c) $i_t = -4^{\circ}$.

Figure 7.- Continued.

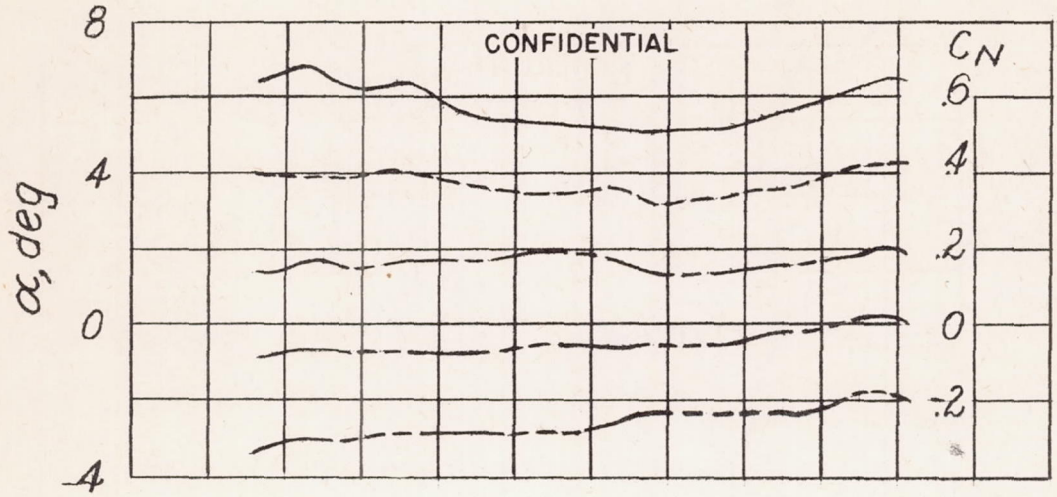

(d) $i_t = 2^{\circ}$.

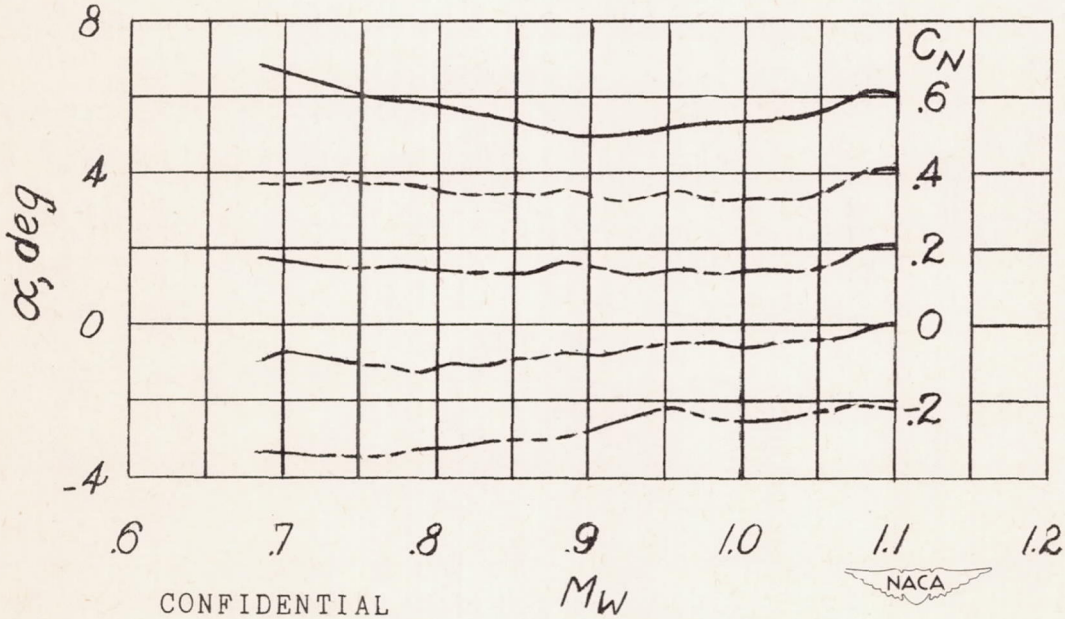

(e) $i_t = 4^{\circ}$.

Figure 7.- Concluded.

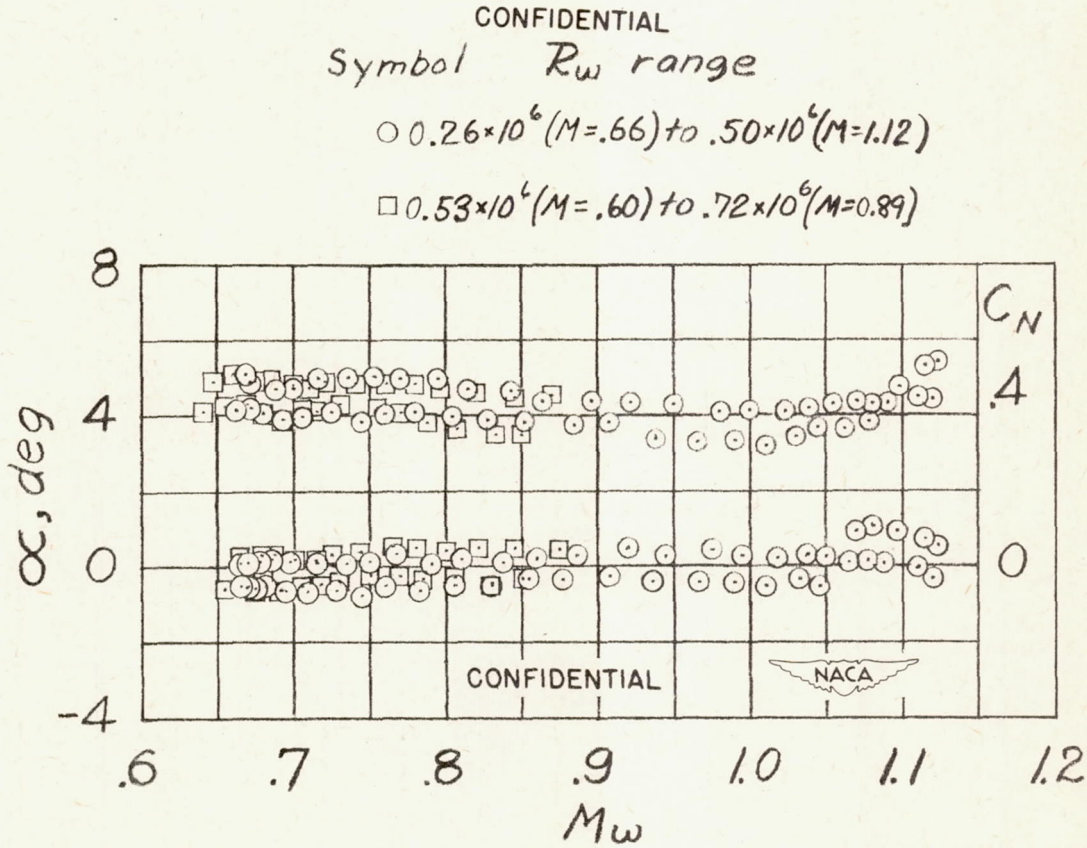

Figure 8.- Typical data showing angle of attack for normal-force coefficients of 0 and 0.4 and two ranges of Reynolds number. $i_t = 0^{\circ}$.

CONFIDENTIAL

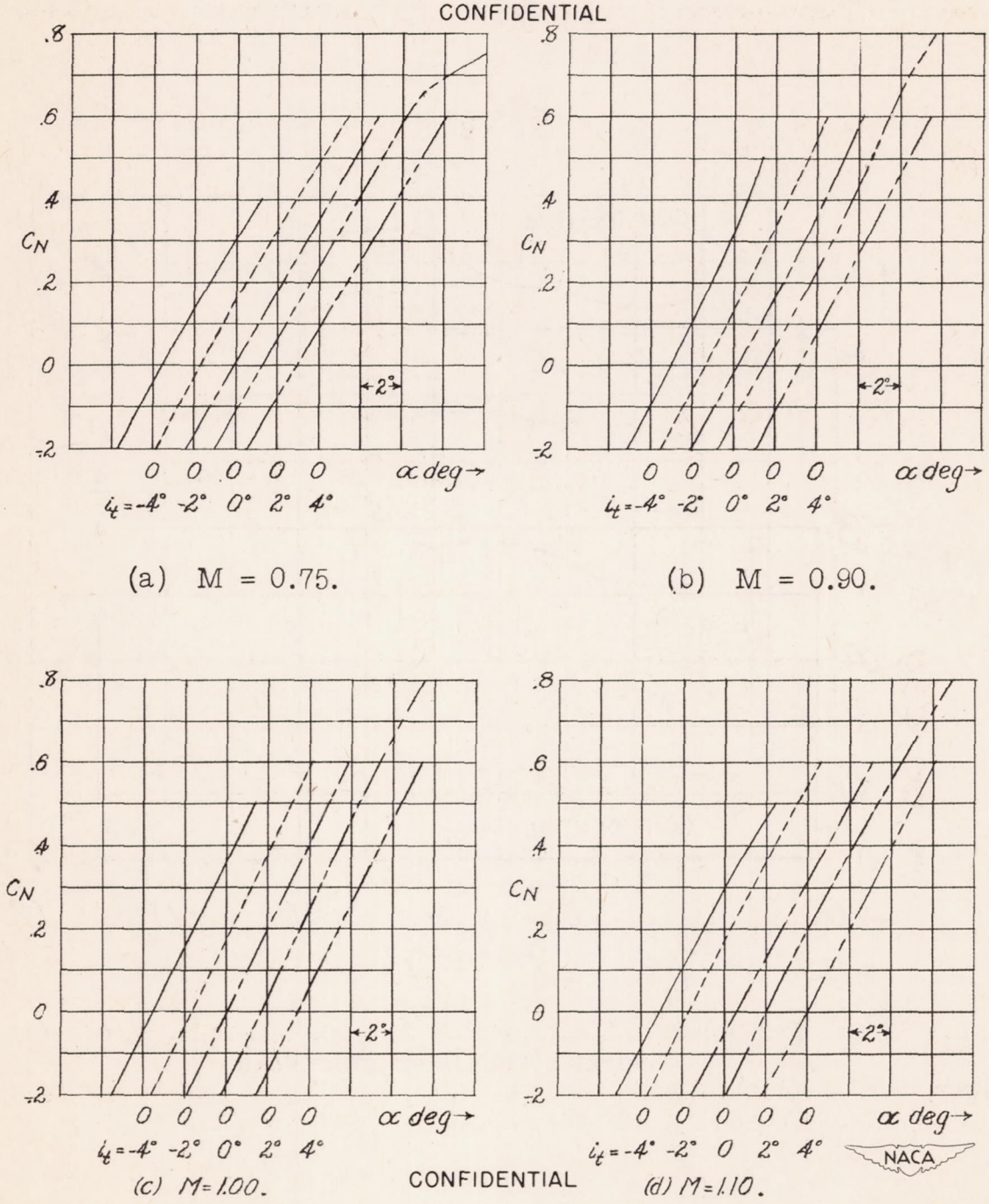

CONFIDENTIAL

Figure 9.- Variation of normal-force coefficient with angle of attack for several stabilizer incidences at various Mach numbers.

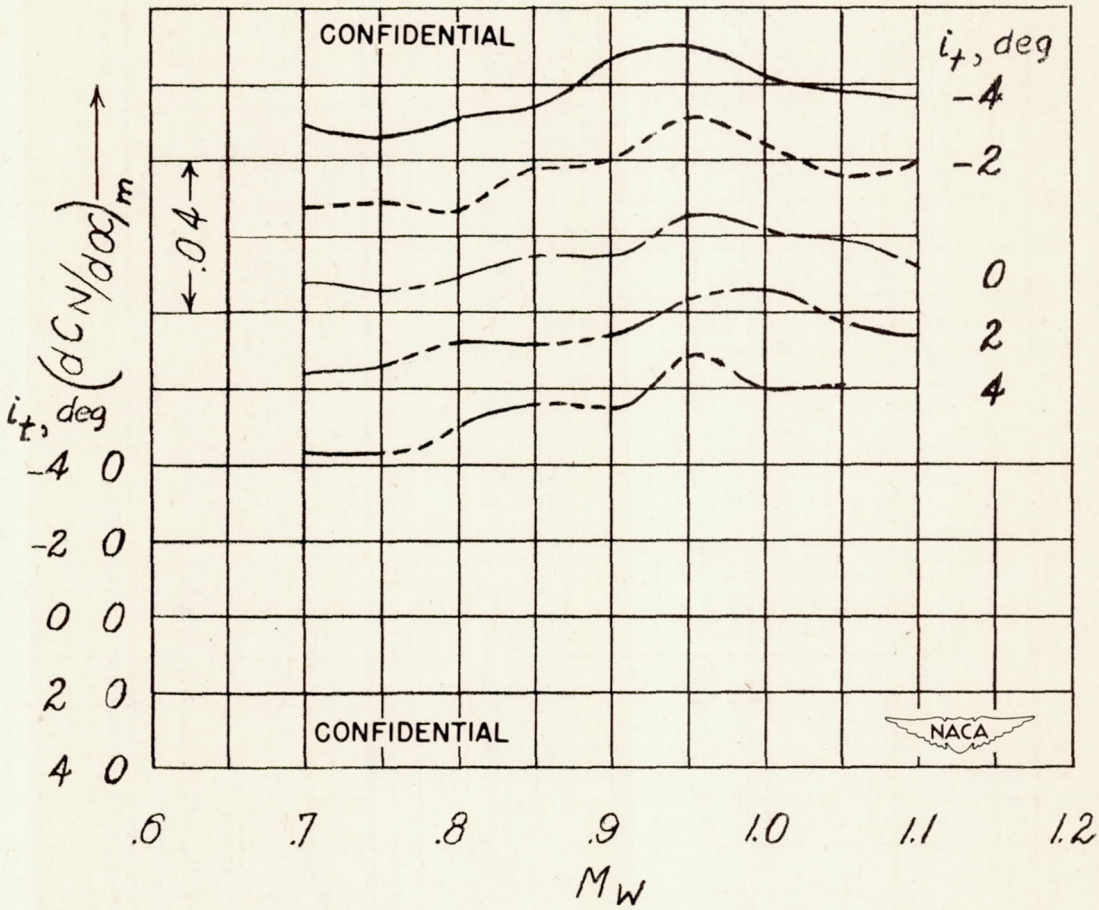

Figure 10.- Variation with Mach number of slope of normal-force curve for various stabilizer incidences.

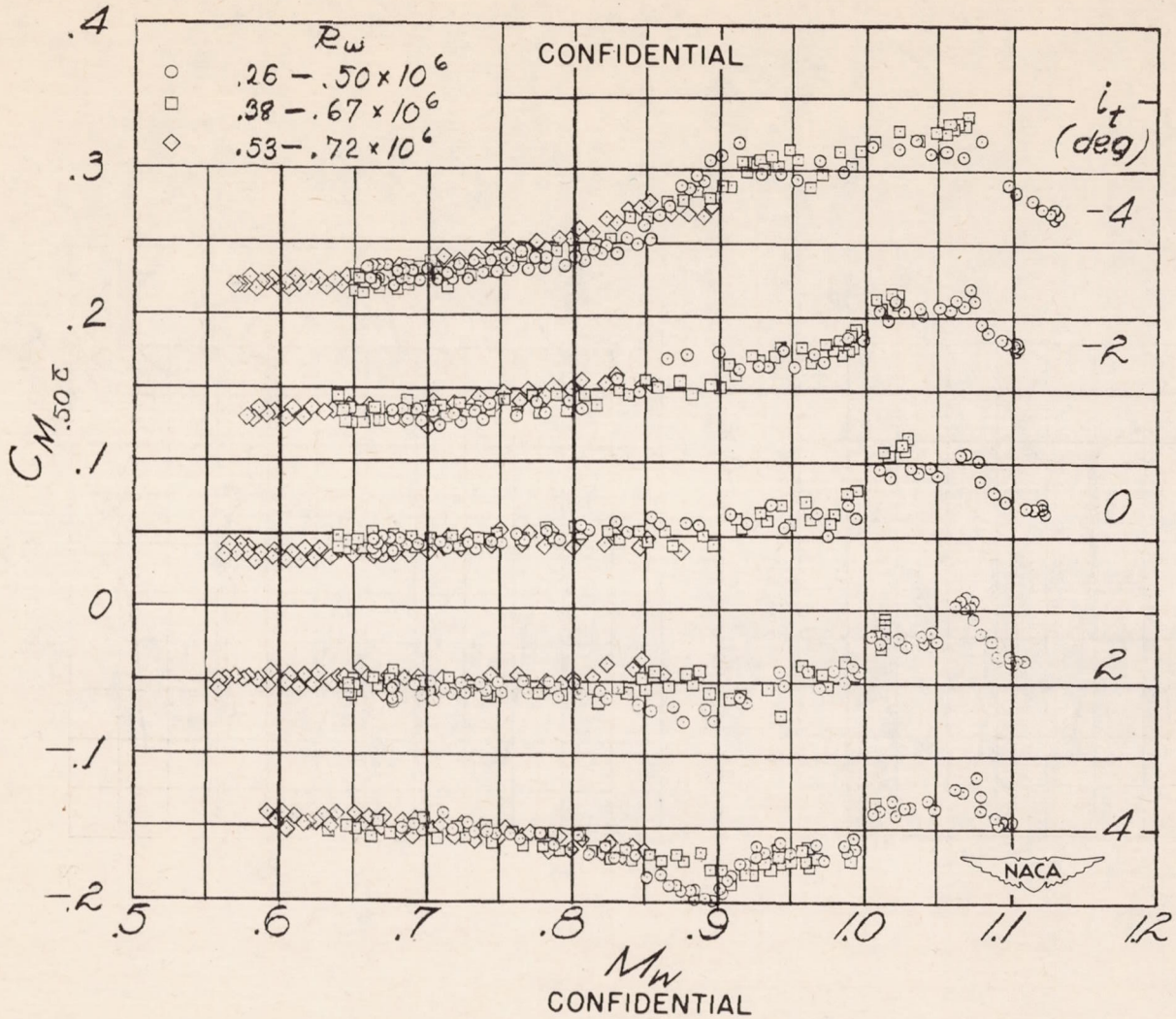

(a) Typical data obtained at three altitudes. $C_N = 0$.

Figure 11.- Variation with Mach number of pitching-moment coefficient at several stabilizer incidences for various normal-force coefficients.

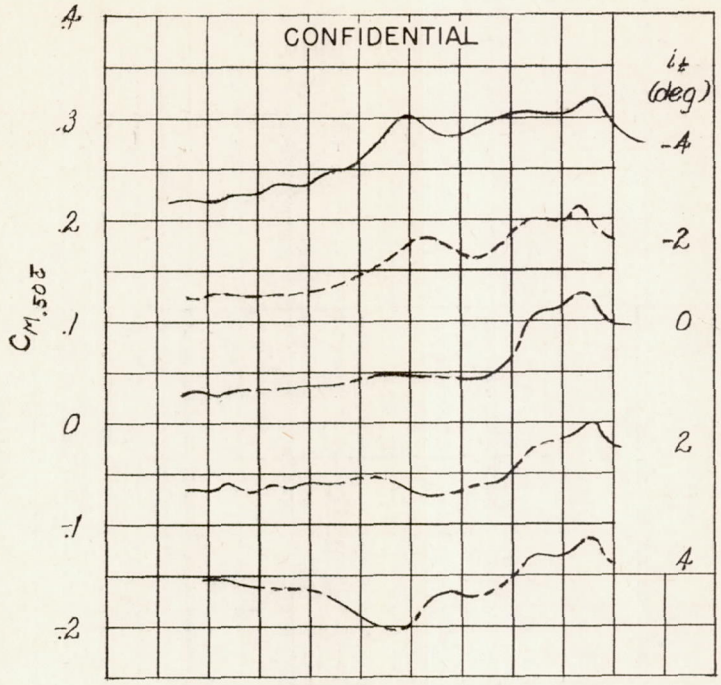

(b) $C_N = -0.2$.

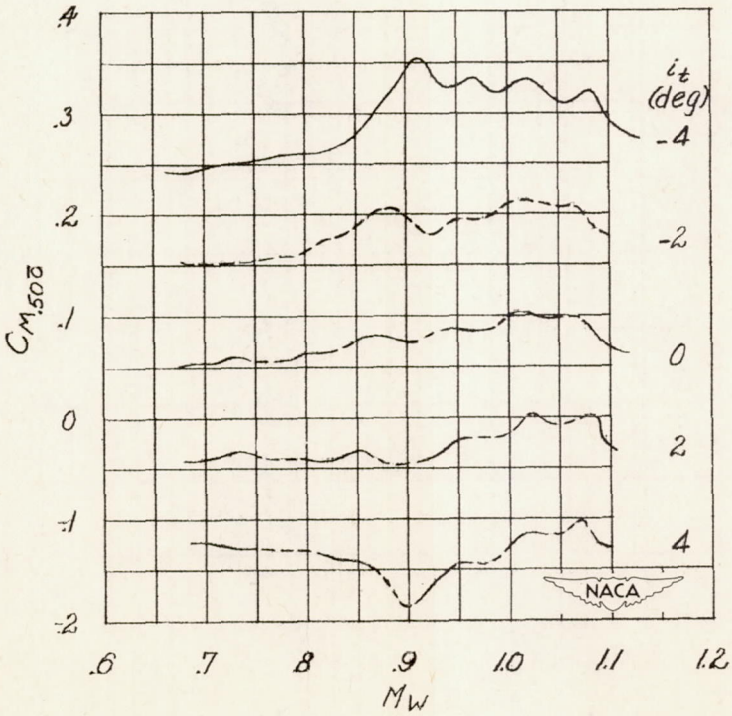

CONFIDENTIAL

(c) $C_N = 0.2$.

Figure 11.- Continued.

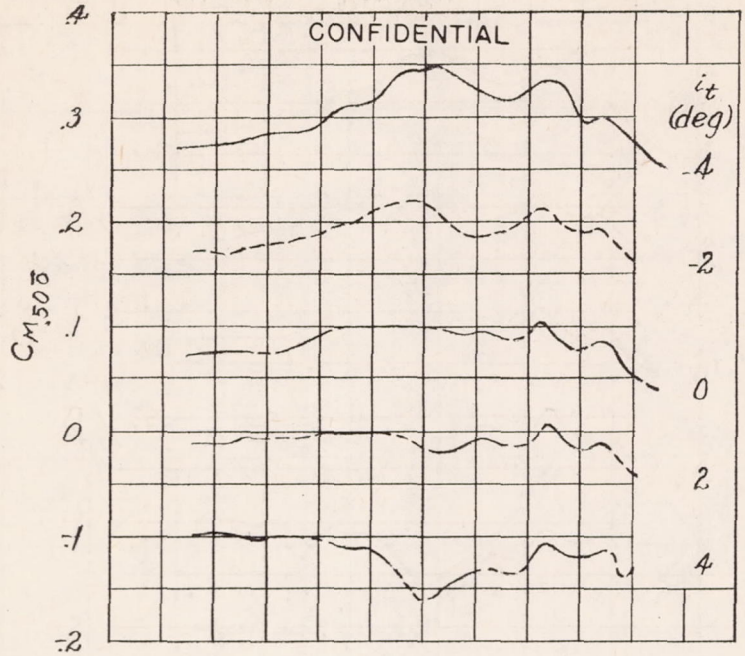

(d) $C_N = 0.4$.

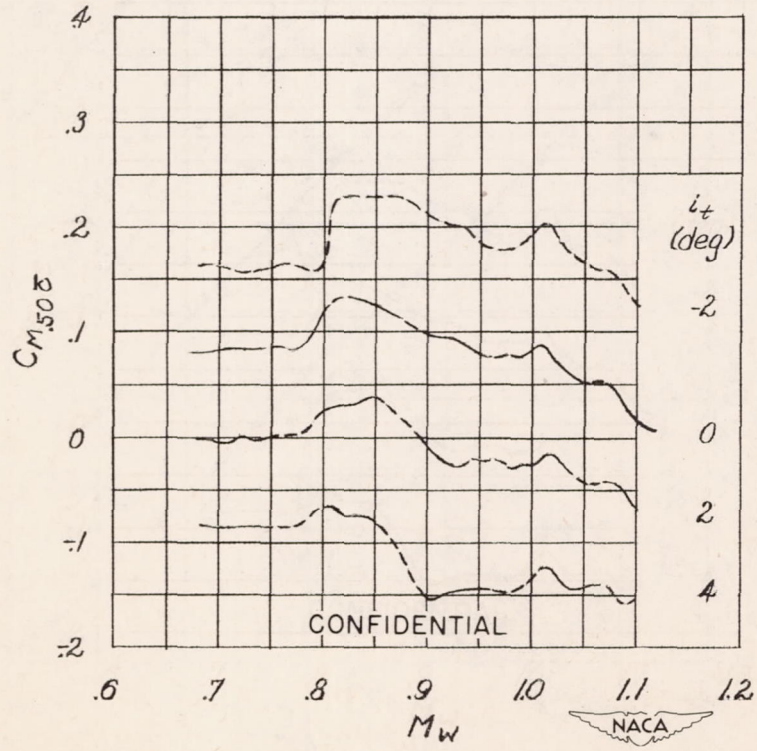

(e) $C_N = 0.6$.

Figure 11.- Concluded.

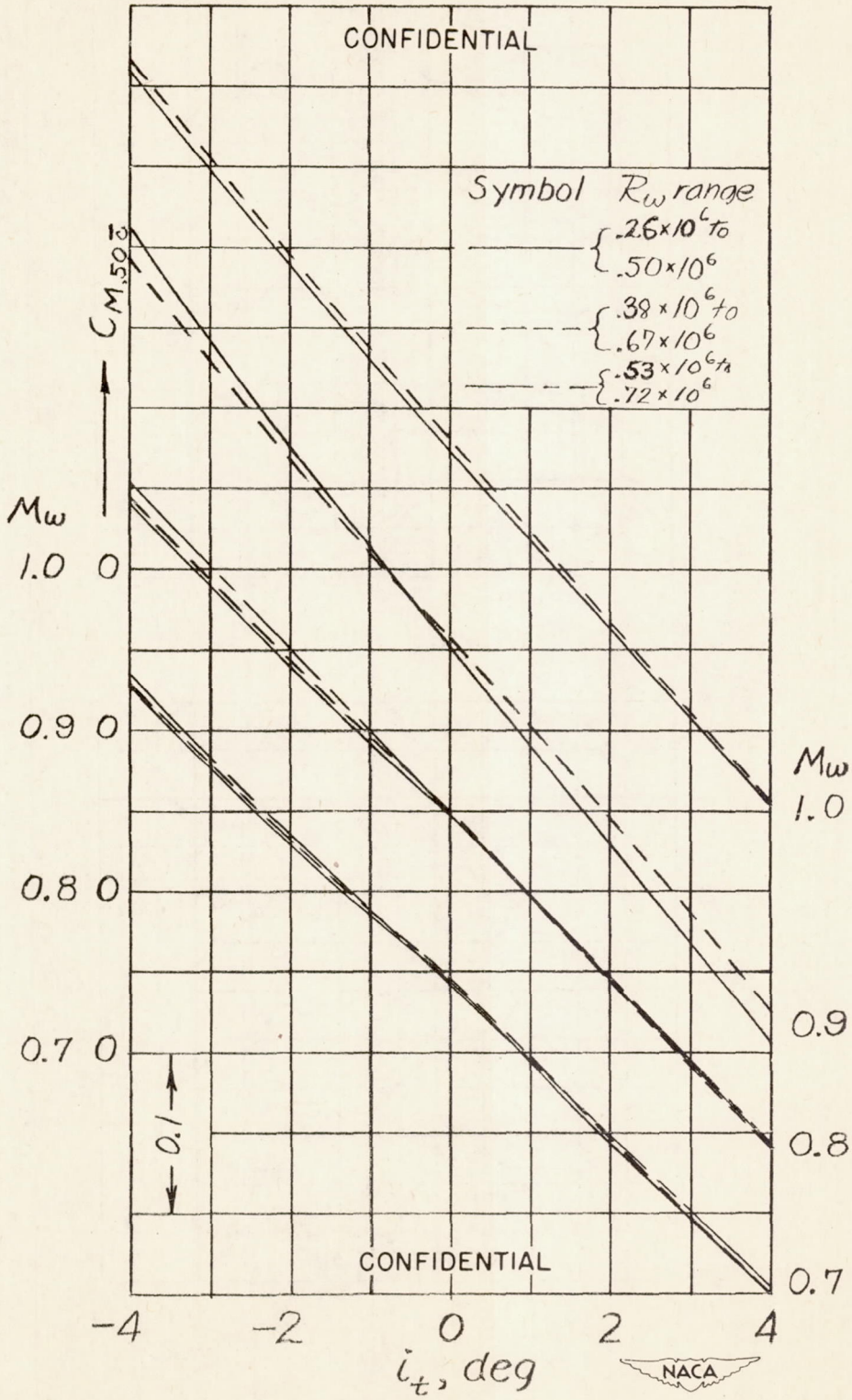

Figure 12.- Variation of pitching-moment coefficient with stabilizer incidence at various Mach numbers for three different ranges of Reynolds numbers. $C_N = 0$.

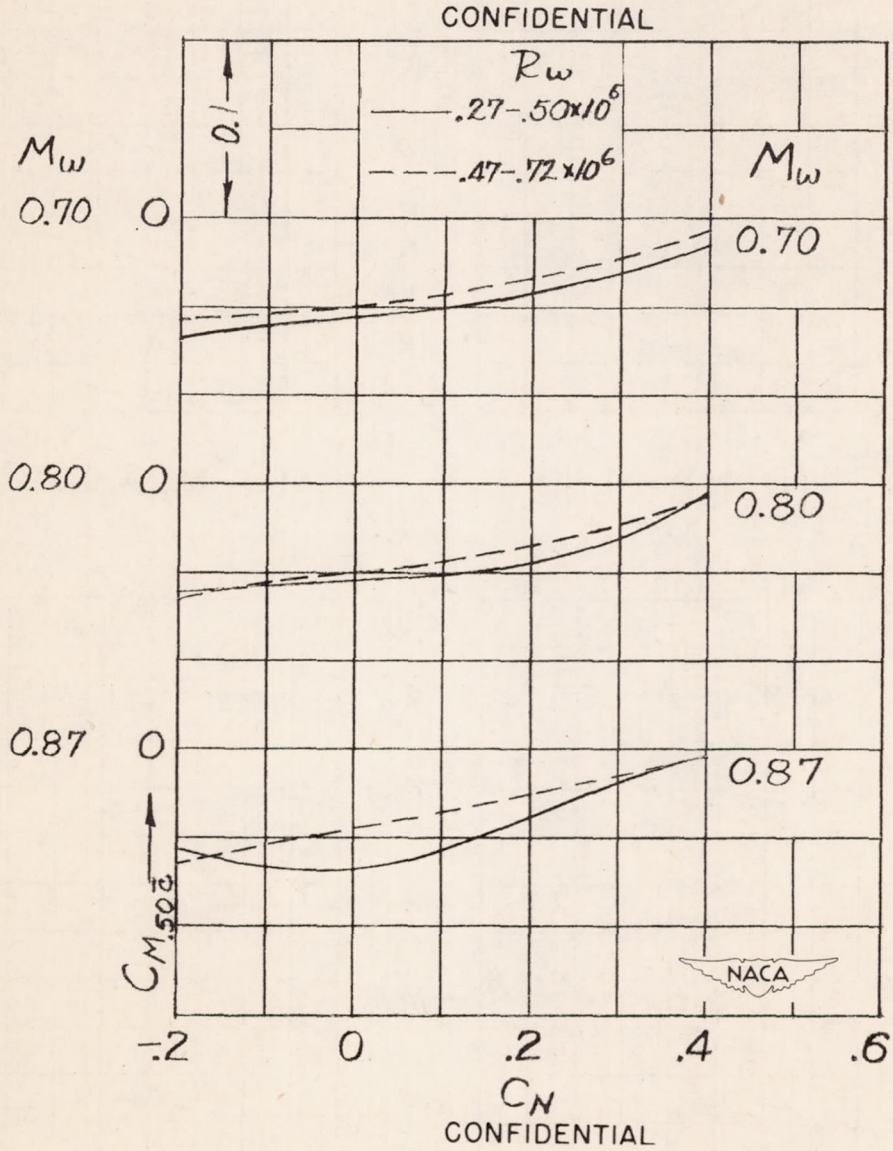

Figure 13.- Variation of pitching-moment coefficient with normal-force coefficient at various Mach numbers for different ranges of Reynolds numbers. $i_t = 2^{\circ}$.

CONFIDENTIAL

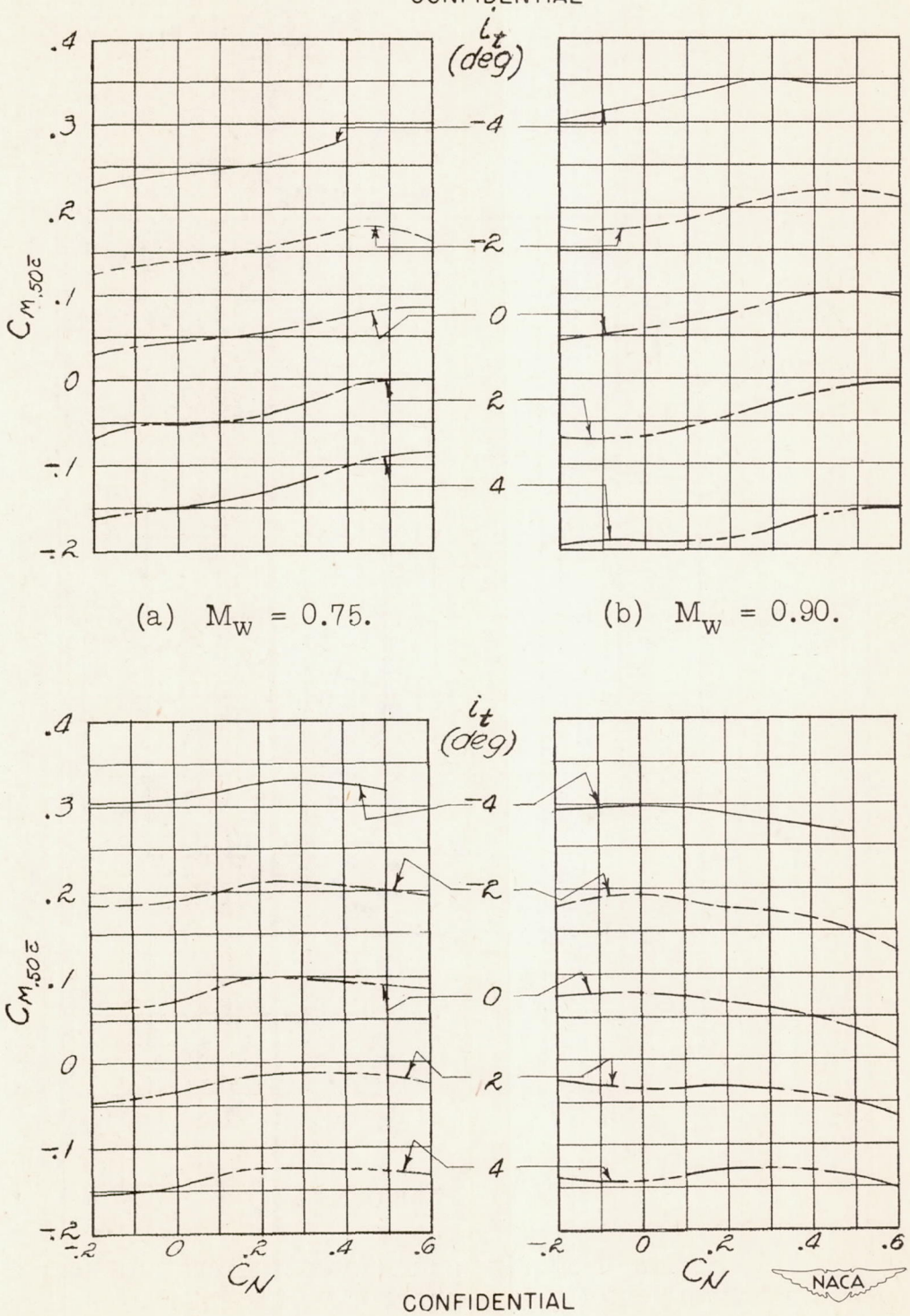

(a) $M_W = 0.75$. (b) $M_W = 0.90$.

(c) $M_W = 1.00$. (d) $M_W = 1.10$.

CONFIDENTIAL

Figure 14.- Variation of pitching-moment coefficient with normal-force coefficient for various stabilizer incidences at several Mach numbers.

CONFIDENTIAL

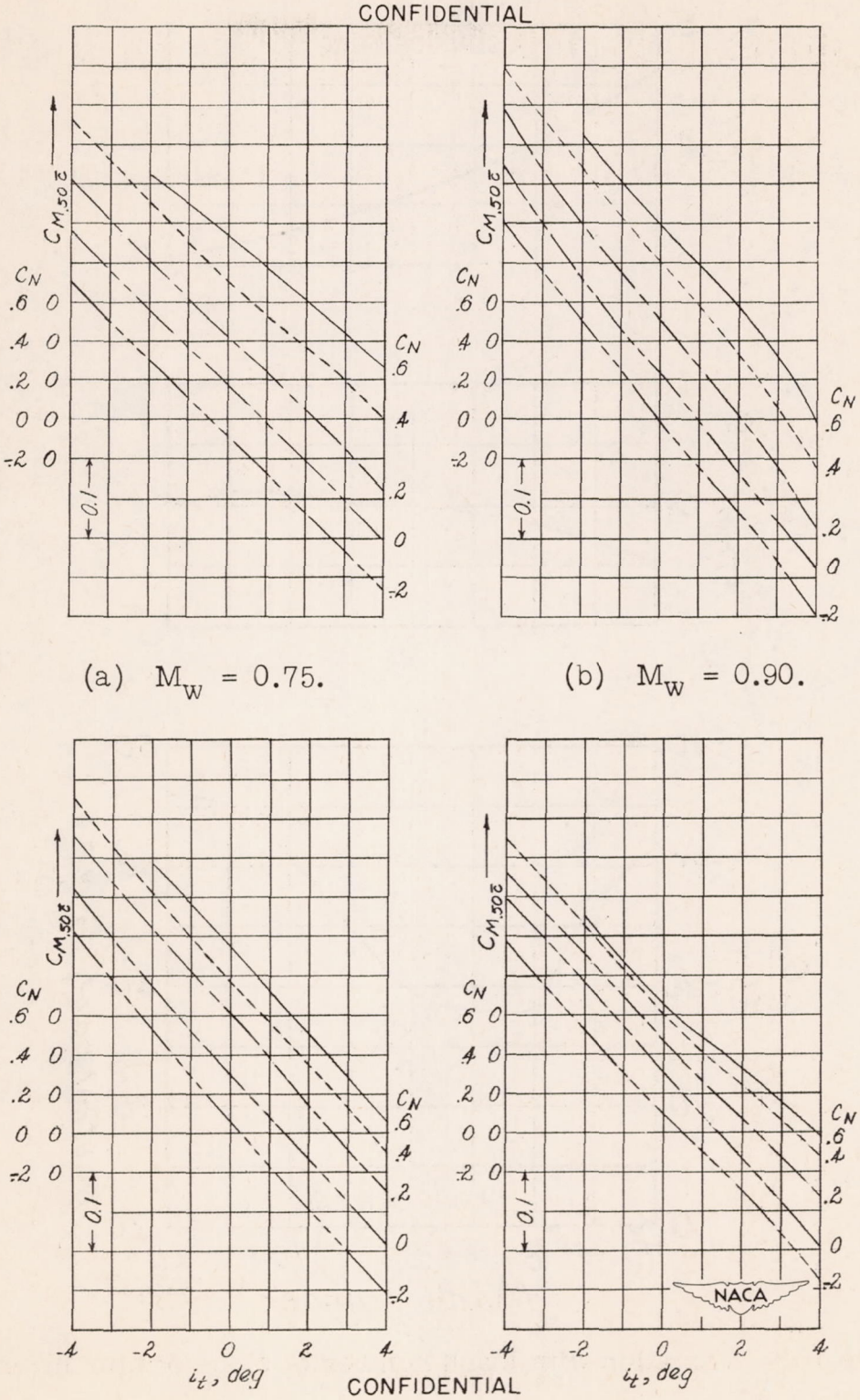

(a) $M_W = 0.75$.

(b) $M_W = 0.90$.

(c) $M_W = 1.00$.

(d) $M_W = 1.10$.

CONFIDENTIAL

Figure 15.- Variation of pitching-moment coefficient with stabilizer incidence for various normal-force coefficients at several Mach numbers.

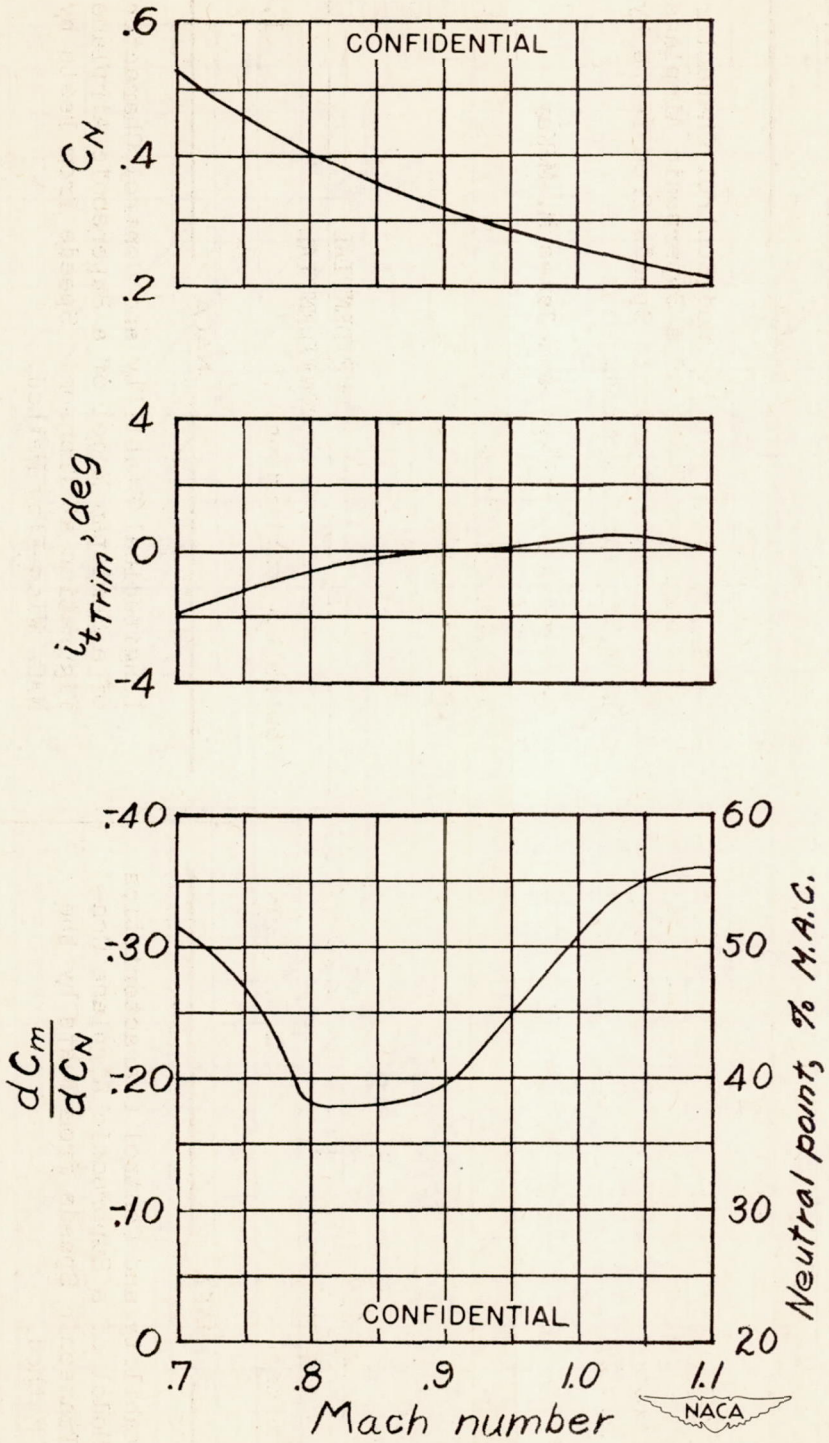

Figure 16.- Variation with Mach number of slope of pitching-moment curve, $\frac{dC_m}{dC_N}$, and stabilizer angle required for trim at altitude of 35,000 feet with wing loading of 90 and center of gravity at 20 percent M.A.C. Normal-force coefficient for level flight also shown.